Science of the Total Environment 755 (2021) 143123

Contents lists available at ScienceDirect

Science of the Total Environment

journal homepage: www.elsevier.com/locate/scitotenv

Profiles and species of Mn, Fe and trace metals in soils near a ferromanganese plant in Bagnolo Mella (Brescia, IT)

Marco Peli [a,*], Benjamin C. Bostick [b], Stefano Barontini [a], Roberto G. Lucchini [c,d], Roberto Ranzi [a]

[a] Dipartimento di Ingegneria Civile, Architettura, Territorio, Ambiente e di Matematica, DICATAM – Università degli Studi di Brescia; via Branze 43, 25123 Brescia, BS, Italy
[b] Lamont–Doherty Earth Observatory, Columbia University; 61 Route 9W - PO Box 1000, Palisades, NY 10964-8000, USA
[c] Dipartimento di Specialità Medico Chirurgiche, Scienze Radiologiche e Sanità Pubblica, DSMC – Università dezgli Studi di Brescia, Viale Europa 11, 25123 Brescia, BS, Italy
[d] Environmental Medicine & Public Health, Icahn School of Medicine at Mount Sinai, 17 E 102 St Floor Third - West Tower, New York, NY 10029, USA

HIGHLIGHTS

- Profiles of potentially toxic elements in soils were investigated near a ferromanganese plant
- Contamination was site-specific and distributed throughout the top 15 cm.
- Manganese (Mn) was independent of other elements and more variable between sites.
- Speciation showed Pb was bound to Mn oxides and As to Fe oxides
- Most Mn was actually found in recalcitrant phases, toxic if tissues—incorporated.

GRAPHICAL ABSTRACT

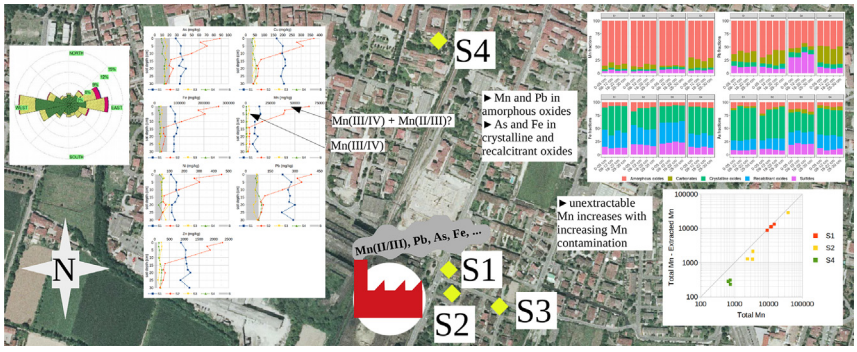

ARTICLE INFO

Article history:
Received 4 July 2020
Received in revised form 11 October 2020
Accepted 13 October 2020
Available online 16 October 2020

Editor: Filip M.G.Tack

Keywords:
Urban soil contamination
Anthropogenic impact
Trace elements
Sequential extraction procedure
Compositional data analysis

ABSTRACT

For the last forty-five years (from 1974 to present) ferroalloy production in Bagnolo Mella, Northern Italy, has generated particulate emissions enriched in potentially toxic metals and metalloids including arsenic (As), lead (Pb) and manganese (Mn). Of these, Mn is unique in that it has a significant background concentration and is seldom studied as a contaminant but is potentially a significant toxin derived from dusts regionally. Here we examine the distribution, redistribution, speciation and bioavailability of the Mn-contaminated top soils affected by atmospheric emissions adjacent to the ferroalloy plant. Four sites, variably located in the study area in terms of both distance and direction from the plant, were considered as representative of increasing levels of industrial influence.

Soil profiles showed that metal concentrations (measured by X-ray fluorescence) varied considerably by location, i.e. higher in the sites closer to the plant and also at the surface level, although distributed throughout the top 15 cm, suggesting appreciable redistribution possibly due to soil mixing or infiltration. Most metal concentrations were correlated, except Mn which was independent and more variable across the sites than the other elements. Sequential chemical extractions indicated that Pb was primarily associated with Mn oxides, while As was most significantly associated with iron oxides.

When Mn concentration significantly exceeded background levels, it was present in phases that were resistant to acid dissolution, very different from typical uncontaminated soils. X-ray Absorption Near Edge Spectroscopy (XANES) analyses suggested this recalcitrant Mn phase is likely a Mn-bearing spinel such as magnetite, that can be particularly toxic if ingested or inhaled.

* Corresponding author.
E-mail addresses: marco.peli@unibs.it (M. Peli), bostick@ldeo.columbia.edu (B.C. Bostick), stefano.barontini@unibs.it (S. Barontini), roberto.lucchini@unibs.it (R.G. Lucchini), roberto.ranzi@unibs.it (R. Ranzi).

https://doi.org/10.1016/j.scitotenv.2020.143123

These first results highlight the legacy of ferroalloy production on surrounding soils, as well as the importance of Mn speciation for soil apportionment evaluation and human exposure estimation.

1. Introduction

Industrial emissions represent important sources of toxic metals and metalloids worldwide, often enriching airborne dust which once deposited represents a possible long-term source of environmental contamination to locally grown vegetables (Ferri et al., 2015), groundwater (Huang et al., 2016), soil (Boudissa et al., 2006) and air through resuspension mechanisms (Layton and Beamer, 2009). The ferroalloy industry, in particular, is a major source of atmospheric emissions of iron (Fe), manganese (Mn) and other elements, and is a significant source of those metals to soils worldwide (Pavilonis et al., 2015). Most studies examining industrial emissions have focused on trace elements like lead (Pb) and arsenic (As), but due to a recently-recognized risk of human health impacts associated with Fe and Mn contamination (Miah et al., 2020; Maher, 2019; Lucchini et al., 2017) active ferroalloy production sites around the world are being investigated to monitor population exposure to Mn (e.g. Otero-Pregigueiro et al., 2018; Fulk et al., 2017). At many other sites where ferroalloy production has ceased, slowed, or has been improved to curb emissions, the environmental risk posed to surrounding communities appears to persist due to historical emissions, but is poorly understood (e.g. Boudissa et al., 2006; Eastman et al., 2013). It is thus critical to study metals accumulated in soils, their redistribution and bioavailability.

Most research has focused on the environmental impacts of emissions by examining the total concentrations of heavy metals and metalloids in dusts or soil (e.g. Tume et al., 2019; Mamut et al., 2018; Urrutia-Goyes et al., 2017). Risks posed by these and other elements to humans and the environment, however, are ultimately determined by the combination of their concentration, solubility and bioavailability (e.g. Sun et al., 2018; Rodriguez et al., 2009). Fewer studies have examined the chemical form of atmospherically deposited emissions in part because assessing chemical forms, and the risks posed by them, requires detailed studies of mineralogy and phase-associations of metals and metalloids, which needs several different methods. Sequential chemical extractions are commonly used measures of metal association, targeting phases' differences in solubility to study both mineral phases and the elements that are associated with them (Davidson et al., 2006). These methods are widely applied and provide invaluable information, despite possible pitfalls as sample artefacts produced through extractions, or non-specific and incomplete dissolution. X-ray absorption spectroscopy or other direct measures of mineralogy and speciation provide direct information about metals but are often not sufficiently diagnostic to differentiate similar phases, such as metals adsorbed on different minerals.

While analysis of published data sets suggests that over 50% of the soils in North America and Europe can be enriched in Mn by anthropogenic sources (Herndon et al., 2011), very little is known about the distribution and chemical forms of this Mn contamination. For example, it is not well known if Mn in soil impacted by anthropogenic atmospheric Mn deposition is mineralogically distinct from natural Mn sources, which are thought to be non-toxic. This distinction is critical to better understand the environmental health risks of deposited and natural Mn phases.

Here, we examine and characterize the extent and speciation of Mn contamination resulting from 45 years of ferroalloy emission in Bagnolo Mella, Italy, the contamination redistribution into secondary mineral phases, and the effect of that potential redistribution on metal bioavailability. We use portable X-ray fluorescence (pXRF) spectroscopy as a rapid, cost-effective screening of in situ soil elemental composition, and link those results to changes in chemical speciation using sequential chemical extractions and spectroscopic approaches (e.g. Hošek et al., 2018), and pedology analyses (e.g. Stockmann et al., 2016). This study, aiming to distinguish the anthropogenic Mn contribution from the natural Mn soil content, represents the first characterization, to this extent, of Mn in soils impacted by ferroalloy production and is useful for risk assessment at historical and current industrial sources. Both the approach and the results of our study are transferable to other industrial sites enriching soil deposition of metals through airborne emissions.

2. Materials and methods

2.1. Site selection

Since the early 1970s, ferroalloy activity in the city of Bagnolo Mella, Northern Italy, has generated particulate emissions enriched in Mn, lead (Pb), iron (Fe), nickel (Ni), copper (Cu), zinc (Zn) and arsenic (As). The factory is located next to the residential area (Fig. 1) in a plain characterised by a shallow surface water table, ranging from 1.5 to 6 m from the soil surface. In the city area, 4 public wells are the extraction points for drinking water (Fig. 1), and they intersect a deeper aquifer at 29–32 m from the soil surface.

After a preliminary evaluation of Mn concentration in surface soils, we identified four sites in the plant's surroundings differently influenced by the industrial emissions (Fig. 2): three of them within 250 m of the emission source (S1, S2 and S3) and the fourth one at a greater distance (S4). The S1, S2 and S3 sites were chosen considering three aspects: (i) close distance from the ferroalloy plant, (ii) downwind position in relation to the prevailing wind blowing West-to-East (see wind rose in Fig. 2), and (iii) soil use, i.e. absence of perturbation. With respect to plant location, S1 is located 103 m far from the plant in the *E*-NE direction, S2 is 88 m and S3 is 206 m far from the plant, both in the E direction, while S4 is located 475 m far from the plant in the N direction (distances measured from the plant chimney to the centre of each site area). Therefore, the three sites S1, S2 and S3 can be considered the most exposed to deposition from airborne emissions, whereas S4 represents a local reference site falling out of the major deposition area due to the combination of distance and direction from the plant.

According to local owners and governmental offices, parts of the soil of all sites were preserved from any construction and maintained as lawns or gardens. This requirement was needed to avoid agricultural disturbances of the soil, enrichment of metals from fertilizers and pesticides use, and simplification of the soil profile (i.e. disruption of the natural horizonation) due to ploughing or tillage practices.

2.2. Field measurement and sampling

Metal concentrations in the investigated sites were measured in situ with a portable X-ray fluorescence (pXRF) instrument (a Thermo Scientific™ Niton™ XL3t GOLDD+ XRF Analyzer), set on Soil Mode. For consistency reasons, every measure was obtained averaging three pXRF readings replicated in the same point. A set of four standard reference materials was measured before each sampling session: SiO_2 (with certified content Mn = Pb = As = Zn = Cu = Ni = Fe = 0), NIST-2709a (Mn = 529 mg/kg, Pb = 17.3 mg/kg, As = 10.5 mg/kg, Zn = 103 mg/kg, Cu = 34 mg/kg, Ni = 85 mg/kg, Fe = 33,600 mg/kg), NCS-73308 (Mn = 1010 mg/kg, Pb = 27 mg/kg, As = 25 mg/kg, Zn = 46 mg/kg, Cu = 22.6 mg/kg, Ni = 30 mg/kg, Fe = 27,000 mg/kg) and GBW-07411 (Mn = 9700 mg/kg, Pb = 2700 mg/kg, As = 205 mg/kg, Zn = 3800 mg/kg, Cu = 65.4 mg/kg, Fe = 56,000 mg/kg). This allowed to consider this method reliable (standards measures were always within 90%–110% of the certified

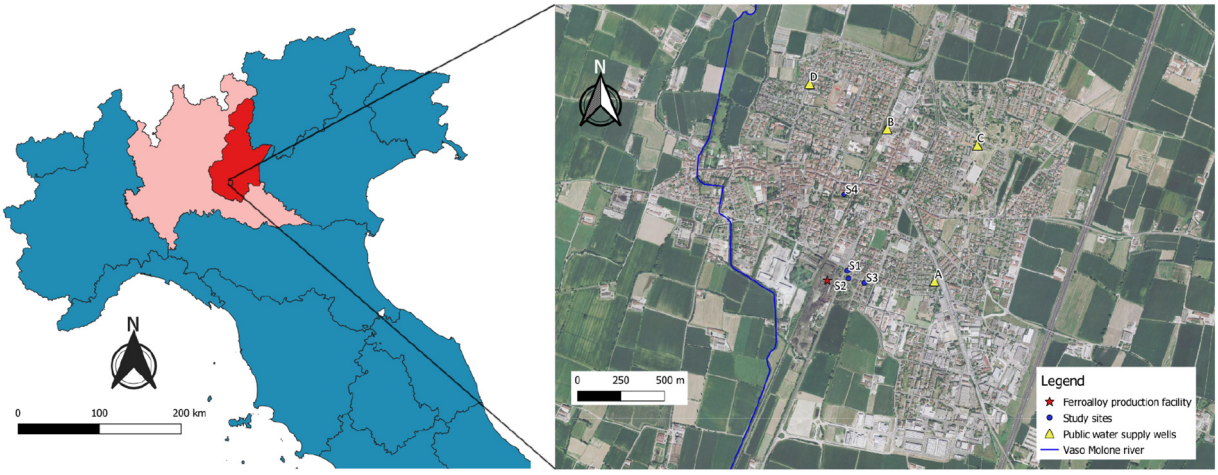

Fig. 1. Location of the study area, with position of the investigated sites, of the ferroalloy production facility and of the public water supply wells in Bagnolo Mella.

values) and to exclude the possibility of Pb interference to As quantification for the values of Pb concentration later measured in the investigated sites.

Each study site was examined using the following suite of measurements: (i) surface elemental composition was measured at multiple locations across the site area for shallow (0–2 cm) samples and in situ pXRF; (ii) in situ pXRF measurements from two soil profiles obtained from sampling 40-cm deep soil pits at 2.5, 5, 10, 14, 18, 20, 25, 30 cm from the surface, both on the clean soil pit floor and (iii) along one vertical wall of each pit; (iv) ~50 g soil samples were collected from each pit at the same depths at which measures at points (ii) and (iii) were taken (± 1 cm); (v) one shallow, undisturbed soil core was taken at each site for laboratory analyses, which were later performed to determine some relevant physical and chemical soil properties (e.g. particle-size distribution, organic matter content and cation-exchange capacity). Statistical analyses, including analysis of variance (ANOVA) and principal components analysis (PCA), of pXRF-measured metal content were performed on logratio-transformed data (Filzmoser et al., 2009) for Pb, As, Zn, Cu, Ni, Fe and Mn, using the *compositions* (van den Boogaart et al., 2019) and *robCompositions* packages in R 3.5.1 (R Core Team, 2018).

2.3. Laboratory analysis

2.3.1. Sequential extractions

Several depth intervals were selected for in-depth analysis using sequential selective extractions. For each interval, four composite samples were prepared from each soil profile at depths consistent with pXRF measurements. These composite samples were subsequently analysed

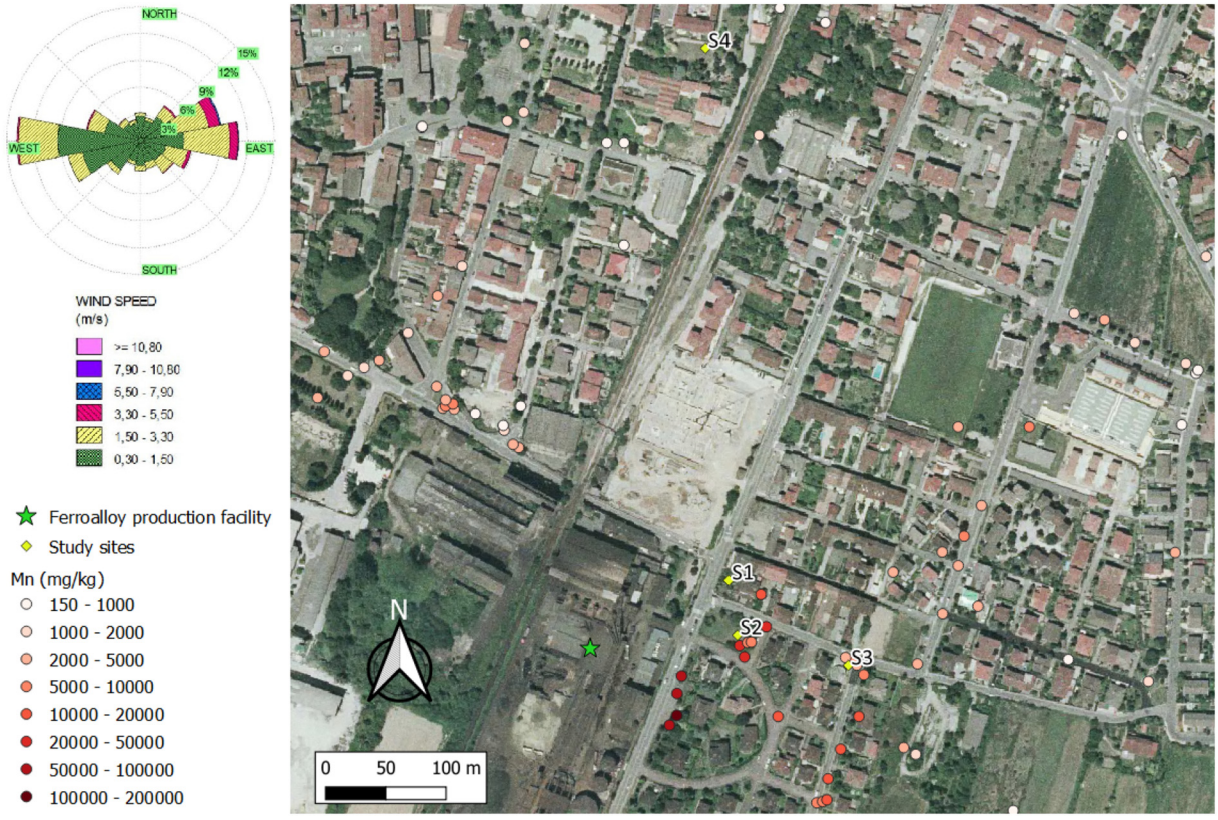

Fig. 2. Focus on the study area with results of the surface soil Mn content preliminary evaluation against the local wind rose from the closest meteorological station, plus location of the ferroalloy production facility and the investigated sites.

by sequential chemical extraction to assess phase associations and bioavailability, and the resulting solutions were analysed using Inductively Coupled Plasma-Mass Spectroscopy (ICP-MS). We used a five-stage extraction procedure based on the work by Sun et al. (**2016a**) and summarized in Table 1. This method, designed and validated in a previous study (Sun et al., 2016b), is particularly well suited to differentiating the most abundant forms of Fe and Mn in soils, and can distinguish between co-precipitated and adsorbed forms of trace elements that can be associated with each phase.

2.3.2. Lung bioaccesibility

We also determined lung bioaccessibility by measuring metal dissolution in artificial lysosomal fluid (ALF) and Gamble's solution (Zereini et al., 2012).

2.3.3. Gastric and intestinal bioaccessibility

We used the method of Basta et al. (2001) to estimate human gastrointestinal bioaccessibility in both syntethic gastric and intestinal solutions.

2.3.4. Extraction procedure

All the extractions were performed on soil samples of 300 mg. The procedure consisted in adding 10 mL of freshly-prepared reactant to the sample, waiting for the prescribed time, between 2 and 48 h, then spinning each sample in a centrifuge at 3250 rpm for 1 min to separate the solid and the liquid phase, before decanting the supernatant into another container for ICP-MS analysis. The residual solids were then washed with 10 mL rinse solution for 10 min prior to additional extraction steps.

To estimate the sequential extraction procedure fractional recovery for each considered metal, the sum of the concentrations extracted in each step was compared with the total content measured by in-situ pXRF analysis (both in mg/kg).

2.3.5. Soil properties analyses

The undisturbed soil sample collected at each site was analysed to determine the soil grain-size distribution, the gravimetric water content in the field w and the residual gravimetric water content w_r, the porosity φ, the bulk density ρ_b, the pH (measured both in water and in KCl), the electrical conductivity EC, the organic carbon content OC and the organic matter content OM (Walkley-Black method), the total nitrogen content N (Kjeldahl method) and the C/N ratio, and the Cation-Exchange Capacity CEC (Mehlich method), all according to Sparks et al. (1996).

2.4. X-ray absorption Near-Edge Spectroscopy (XANES)

XANES is diagnostic of oxidation state and mineralogy and can be performed on soils without treatment or isolation. Manganese K-edge XANES spectra were collected for the soil profile that was highest in Mn at the Stanford Synchrotron Radiation Laboratory (SSRL) on beamline 4–1. Data were collected in fluorescence mode using a He-filled ion chambers to measure incident and transmitted beam intensity, and either a 13-element Ge detector or a PIPS (planar implanted passivated silicon) detector to measure fluorescence. Normalized fluorescence spectra (fluorescence divided by incident intensity) were calibrated by setting the first inflection point of the Mn foil to 6539.0 eV. XANES spectral analysis involved energy calibration, background subtraction, and normalization, and then quantification by comparison or linear combination fitting (LCF) with reference spectra. LCF was done with the software package Sixpack (Sam Webb, SSRL) using the 6525–6570 eV XANES region of the spectrum. Our final fits contained contributions from $MnCO_3$, $MnHPO_4$, Mn_2O_3, Mn_3O_4, $(Mn, Fe)_3O_4$, δ-MnO_2 (birnessite). Other phases, including MnO, $MnSO_4$, MnO_2 (pyrolusite), and $Ba(Mn^{2+})(Mn^{4+})_8O_{16}(OH)_4$ (approximate formula, psilomelane) were considered but not necessary for fitting. Goodness-of-fit is estimated using the R-factor and reduced χ^2. Error estimates from fitting were calculated by SixPack and are based on sensitivity of results, spectral quality of samples and reference spectra, and spectral uniqueness. In most cases, errors were 5% of total Mn or less.

Table 2
Soil properties of the investigated sites.

		S1	S2	S3	S4
Skeleton	g/kg	213.60	48.90	380.5	272.7
Sand	g/kg	622.00	647.75	659.20	583.00
Silt	g/kg	217.20	181.15	84.60	224.40
Clay	g/kg	160.80	171.10	256.20	192.60
Water content w	g/g %	16.00	16.42	12.67	15.84
Residual water content w_r	g/g %	1.35	1.78	0.96	1.43
Porosity φ	cm3/cm3	0.61	0.63	0.61	0.67
Bulk density ρ_b	g/cm3	1.034	0.992	1.036	0.884
pH (in H_2O)	–	8.06	8.07	8.10	8.01
pH (in KCl)	–	7.39	7.36	7.54	7.34
Electrical conductivity EC	mS/cm	0.127	0.173	0.109	0.107
Organic carbon OC	g/kg	22.45	27.09	15.00	30.72
Organic matter OM	g/kg	38.61	46.59	25.80	52.84
Total nitrogen N	g/kg	2.67	3.18	1.76	2.83
C/N ratio	–	8.41	8.52	8.52	10.85
Cation-Exchange Capacity CEC	meq/100 g	15.36	17.06	15.78	19.32

3. Results and discussion

3.1. Soil properties and metal concentrations across sites and depths

All sites were relatively similar in soil grain-size distribution and basic chemical and hydrological properties (Table 2). The soils are all slightly alkaline with a sandy loam or sandy clay loam soil texture, while their organic matter content OM varies in the range 25–50 g/kg, with OM(S3) < OM(S1) < OM(S2) < OM(S4). Despite this relative homogeneity in soil characteristics, the total metal concentrations varied significantly ($p = 0.001$) between sites according to the ANOVA analysis (Table 3), and displayed generally decreasing levels of metals with soil pit depth (Fig. 3).

In order to compare the measured concentrations with geochemical background values and thresholds for the identification of unusually high element concentrations, due to the absence of locally established values, data reported by both Blume et al. (2016) and Riemann et al. (2018) were taken into consideration.

In the control site S4, soil elemental concentrations changed little with depth, and had values within most of the considered background ranges across the whole soil profile for all the considered elements. The same can be seen in S3, with the exception of Mn showing an enrichment in the top 5 cm of the soil profile. Site S1 showed a variable

Table 1
Steps of the applied sequential extraction procedure, modified from Sun et al. (2016a).

Step	Extractant	Time	Target Mn and Fe phases
1	1 mol/L sodium acetate $C_2H_3NaO_2$ adjusted to pH 4.5 with acetic acid CH_3COOH	24 h	Mn and Fe carbonates
2	1 mol/L hydroxylamine-hydrochloride $[NH_3OH]Cl$ in 25% v/v acetic acid CH_3COOH	48 h	Amorphous Mn and Fe(III) oxides
3	50 g/L sodium dithionite $Na_2S_2O_4$, pH 4.8 with acetic acid CH_3COOH	2 h	Crystalline Mn and Fe(III) oxides
4	0.2 mol/L ammonium oxalate $(NH_4)_2C_2O_4$ / 0.17 mol/L} oxalic acid $C_2H_2O_4$	6 h	Recalcitrant Mn and Fe oxides
5	16 mol/L nitric acid HNO_3	2 h	Mn and Fe(II) sulphides

Table 3
Statistical summary of pXRF-measured soil metals concentrations (mg/kg) with output of the ANOVA analysis; [x]: mean values of the same metal which are followed by the same letter are not significantly different at p = 0.001 across the investigated sites.

		Pb	As	Zn	Cu	Ni	Fe	Mn
	Min	150.2	15.01	577.9	111.7	48.73	37,147	4470
S1	Max	408.3	52.91	1581.1	263.0	216.72	102,071	18,249
(43)	Mean[x]	254.7 a	33.89 a	1015.3 a	192.8 a	132.02 a	78,117 a	11,487 a
	SD	55.84	8.56	222.34	34.59	33.76	17,113.13	3147.55
	Min	62.92	11.95	109.9	26.10	25.89	21,953	881.6
S2	Max	452.23	109.76	2580.0	440.70	533.18	306,448	79,095.5
(55)	Mean	223.96 a	46.83 b	1123.5 a	190.56 a	203.97 b	121,858 b	23,627.4 b
	SD	123.94	27.35	818.78	125.27	144.13	88,173.41	21,751.88
	Min	33.76	6.75	62.31	16.40	23.62	10,661	634.6
S3	Max	98.82	22.19	321.69	74.08	137.22	41,966	5126.6
(49)	Mean	64.11 b	14.74 c	193.14 b	44.91 b	55.10 c	26,152 c	2418.5 c
	SD	14.80	3.43	54.07	11.80	23.89	6114.39	1100.76
	Min	38.59	4.08	99.18	24.18	21.37	9592	424.9
S4	Max	133.36	24.95	278.72	69.72	87.95	30,260	938.4
(57)	Mean	73.16 c	11.34 d	167.56 c	42.91 b	43.18 c	19,354 d	692.5 d
	SD	20.11	3.35	45.89	11.07	17.22	3530.17	101.81

trend, with a maximum soil concentration observed at 15–20 cm below the soil surface for As, Fe, Pb and Zn, while the maximum Mn concentration was observed at 5 cm depth. Finally site S2 showed the same trend for all the considered metal: a significant enrichment in the top 5 cm and concentrations decreasing with depth until close to the background values around 15 cm depth. In general, the concentrations of Cu, Fe, Mn, Pb and Zn at the more contaminated sites S1 and S2 (top 15 cm) are all elevated relative to the considered background values. As and Ni differ from the other elements as their concentrations in site S1 fall within some of the highest background values proposed in the literature, while in S2 they fall outside the background range only in the top 5–10 cm. The elevation of Mn concentrations at or near the surface in these profiles (except S4) is consistent with an additional Mn source (emissions) at these sites. Such Mn enrichment is also found in areas surrounding the ferroalloy production facility in Marietta, Ohio, USA (Carter et al., 2015). We can estimate the surface Mn enrichment at sites S1-S3 by calculating the ratio of mean Mn content in those sites relative to local background levels at the control site S4 and in deeper soil samples. We find that surface soils at contaminated sites S1-S3 are enriched in Mn by 18-, 80- and 5-fold respectively. These indicate Mn deposition is highly heterogeneous and focused mostly within 500 m from the ferroalloy production site. The enrichment ratios in this study are similar to or higher than those reported by Carter et al. (2015) for another ferroalloy production facility, consistent with their locations being somewhat closer to industrial activities. Other metals also appear to be highly enriched and following similar trends with depth.

Overall, these data show that the study area is influenced by one, or more, atmospherically-derived source of Mn, Pb and other contaminants, and that these contaminants have been transported or mixed to some extent into the soil profile. This depth distribution is somewhat unexpected because the metals are insoluble and thus often persist where they are deposited, at the soil surface (Lambert and Lane, 2004). Deviations in their depth distribution are more consistent with downward transport induced by soil mixing, colloid transfer, or potentially biological cycling (Kaste et al., 2011). Differentiating between these is possible by comparing the pattern of downward transport for each of the metals.

The Principal Component Analysis (Fig. 4) performed on the 7 contaminant metals at each of the contaminated sites (S1-S3) indicate that there are two distinct principal components (PC1 and PC2) needed to describe metal concentrations (explaining >80% of variance). PC1 has high Mn loading, and PC2 has high Ni, Cu, Zn and/or As loading. The chemical characterization of these two PCs became stronger when the entire dataset (204 measures in the 4 sites, including the control site) was combined for analysis. The complete dataset was described well (>80% of variance) by two principal components, with PC1 dominated by Mn and two different groups of elements contributing to PC2. The first PC had high Mn loading and lesser amounts of Pb; the second PC was composed of higher Ni-Zn-Cu-Pb and, to some extent, Fe and As. In contrast, the control site S4 did not show clusters with distinct chemical composition.

The separation of Mn from other elements into a single PC suggests either a different contamination source, and/or process involved in downward migration through the soil profile. The strong overall association of Ni, Cu, Zn and Pb is expected as they are divalent chalcophiles, and suggest that they all have a common source, however, the differentiation of Ni, Cu, and Zn from Pb (into PC1) and of As (which is associated with Fe) indicates that these elements are likely repartitioning in the soil due to adsorption. These trends are expected as Pb preferentially is adsorbed on Mn oxides (Villalobos et al., 2005) and As adsorbed strongly to Fe oxides (Dixit and Hering, 2003). These metals are commonly adsorbed on organic matter too, but extractions suggest that these organically-complexed metals are present but less abundant than mineral forms, and they do not vary with organic matter content; this last aspect can be seen also in this case, given the very similar organic matter content and pH between the more impacted site S2 and the control site S4. The lack of clear association of Fe in either PC indicates that it is equivalent in most samples, likely if it is soil-derived rather than a contaminant.

3.2. Phase associations of Mn and other trace elements

The applied sequential chemical extraction procedure allowed to differentiate As, Fe, Mn and Pb in different mineralogical pools: (i) carbonates, (ii) amorphous oxides, (iii) crystalline oxides, (iv) recalcitrant oxides and (v) sulphides (Fig. 5). Commonly, carbonates and sulphides can be associated with elements of lithogenic origin, while oxides can be associated with both pedogenic processes and atmospherically derived anthropogenic contamination (Blume et al., 2016).

When Mn concentrations were at or near background levels, most of the extracted Mn was present in HCl-extractable pools, operationally defined as amorphous oxides, with a less important ratio extracted in carbonates. HCl-extractable Mn was essentially constant with depth and across the sites. Thus, the prevalent form of Mn in local soils appears to be largely present as acid-soluble Mn(III/IV) oxides such as birnessite. This is largely expected, as birnessite is abundant in oxidize surficial soils. In more contaminated sites, however, Mn was often also poorly extracted. At site S3, Mn is also extracted in the sulfide fraction, though the presence of sulfides cannot be confirmed. At the most contaminated sites (S1 and S2), as much as 85% of the total Mn was not extracted (Fig. 6). Therefore, Mn contamination appears to be primarily associated with a phase that is not extracted with conventional extraction procedures.

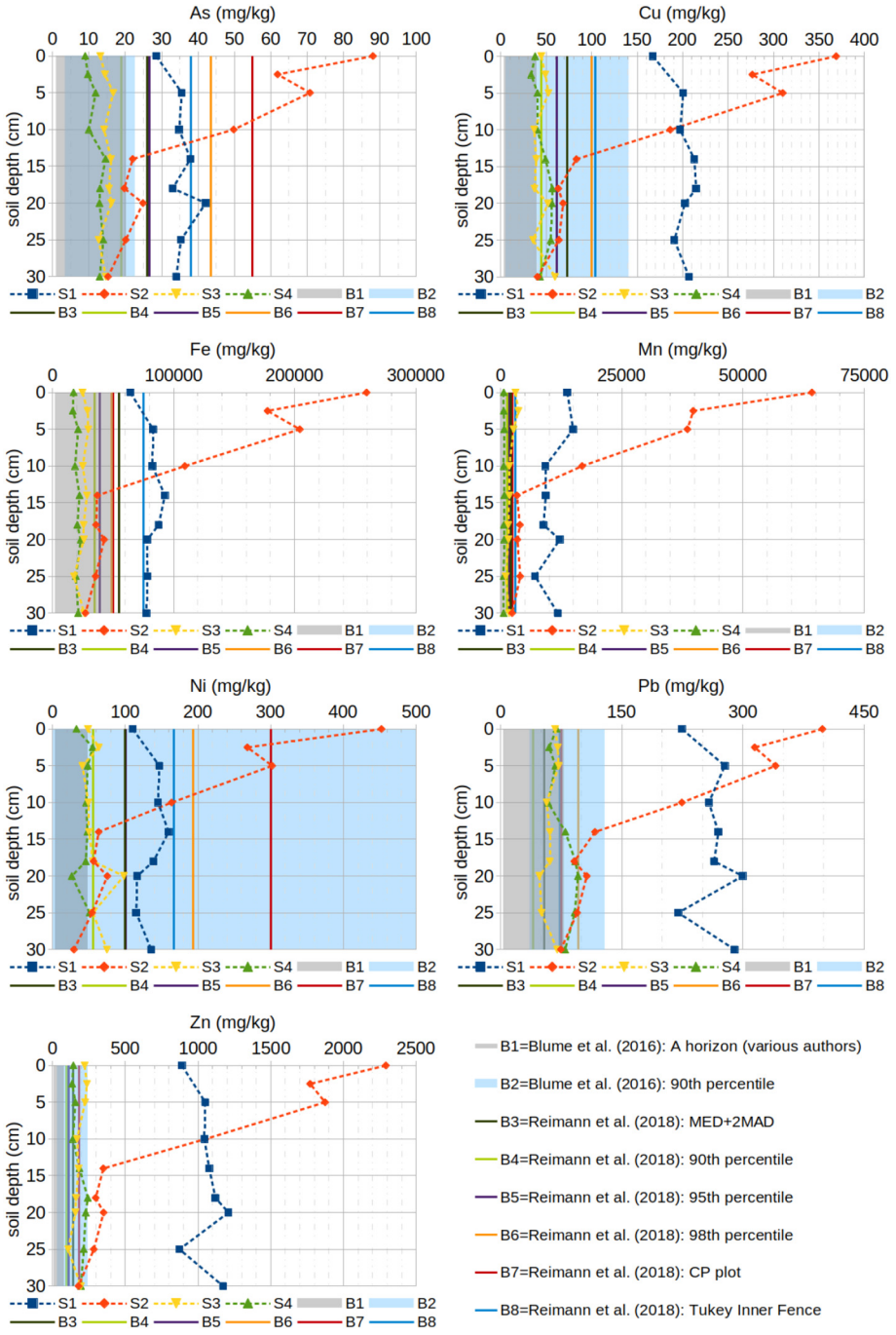

Fig. 3. Average distribution of (pXRF-measured) potentially toxic elements with soil depth in the investigated sites. Background ranges B1 and B2 from Blume et al. (2016), thresholds B3-B8 proposed by Reimann et al. (2018) for the identification of samples with unusually high element concentrations in Southern Europe.

Pb also was largely HCl-extractable, suggesting it was associated with Mn (and potentially some Fe) oxides. On the other hand, Fe was mostly extracted in crystalline and recalcitrant oxides (goethite, hematite and possibly magnetite), with very little extracted in HCl-soluble forms such as the amorphous iron hydroxide ferrihydrite. Consistently with Fe, most As was extracted in the crystalline and recalcitrant oxides pool. This strong association of Pb with amorphous Mn oxides, and of As with Fe oxides is commonly observed in soils (Trueman et al., 2019), especially at circumneutral pH where adsorption is most extensive. The repartitioning of trace metals with Fe and As, while not unexpected, indicates that the soil controls the chemical form and solubility of these metals, not the source, with the exception of Mn in contaminated environments, which has a distinct form representative of the contaminant source. Given the observed downward migration in soil profiles, it is possible that this redistribution results from partitioning onto soil minerals, but it also could be occurring through colloid transport after adsorption to Fe and/or Mn.

The insoluble form of Mn in our study in Bagnolo Mella deserves special attention. Not only is this form different from controls, but it appears to be distinct from other nearby contaminated sites. For example, Mn contamination appears to be primarily associated with the reducible mineral fractions in Vallecamonica, a wide (4748 km^2) area in the northern part of the Brescia province where there was extensive historical ferroalloy production (Borgese et al., 2013). Thus, it appears that there are mineralogical changes that occur in soils that render Mn more soluble, and likely affect its biological effects, over time.

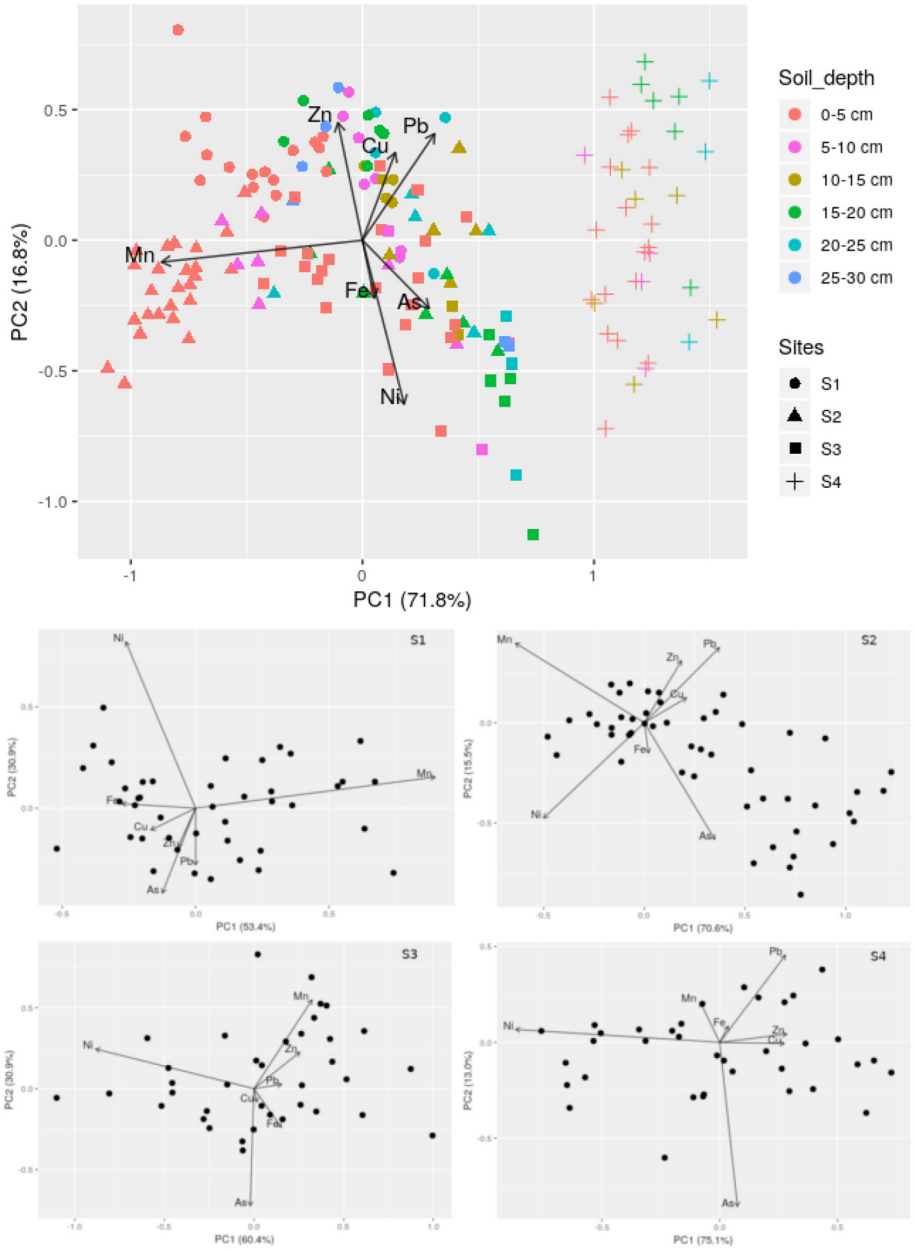

Fig. 4. Biplot of the principal component analysis on the whole dataset and on the site-specific datasets. Considering the whole set, two PCs are sufficient to explain most (88.4%) of the data variability, metals contribute to PCs definition in three groups.

3.3. XANES analysis

X-ray absorption spectroscopy is useful to characterize this insoluble fraction, and to differentiate it from more soluble forms of soil Mn. Our results (Fig. 7) indicate that Mn in contaminated soils from Bagnolo Mella is not in the Mn(IV) forms that are common in soil but instead contains a mixture of Mn(II) and Mn(III) oxidation states and has a spectrum similar to Mn-substituted magnetites. The $(Mn,Fe)_3O_4$ reference spectrum has all the spectral features present in the shallower soil samples, but with sharper features than the soils. We interpret this difference as evidence that the ratio of Fe replaced by Mn in our samples is more extensive than 20%, which is the amount in our reference sample (Liang et al., 2014). There are minor components of MnOOH and MnO_2, both of which are abundant at depth, though accurately assessing their fractional concentrations by LCF is difficult because of the prevalence and peak shape of $(Mn,Fe)_3O_4$. This is consistent with sequential extractions in that these phases are stable and relatively insoluble under most conditions. Magnetite is a common product of fuel combustion and steel production (Maher et al., 2016), and we thus interpret this magnetite phase as a primary signature of ferroalloy emissions impacting soil Mn. This $(Mn,Fe)_3O_4$ phase is also present at 15 cm depth. Given that it is difficult to form Mn-substituted magnetites in soils at low temperatures, their presence at depth indicates that they are being transported through the soils as colloids. Given the differences in extractions of soil Mn for contaminated sites in Valcamonica, it is likely that these phases convert to other mineral forms over time. Future studies should include additional XANES measurements to study these unique components further, and to more conclusively link mineralogical changes to changes in Mn reactivity and potential toxicity in sites of current or historical ferroalloy production. Such analysis might help to differentiate the contaminated and background soils based on their relative content of Mn(III) oxyhydroxides and the Mn(III/IV) oxide birnessite, which both are HCl-extractable (Rico et al., 2009), and of the mixed Fe—Mn magnetite $(Fe,Mn)_3O_4$, which is the major form of Mn in still mill dusts and whose nanoparticles are known to

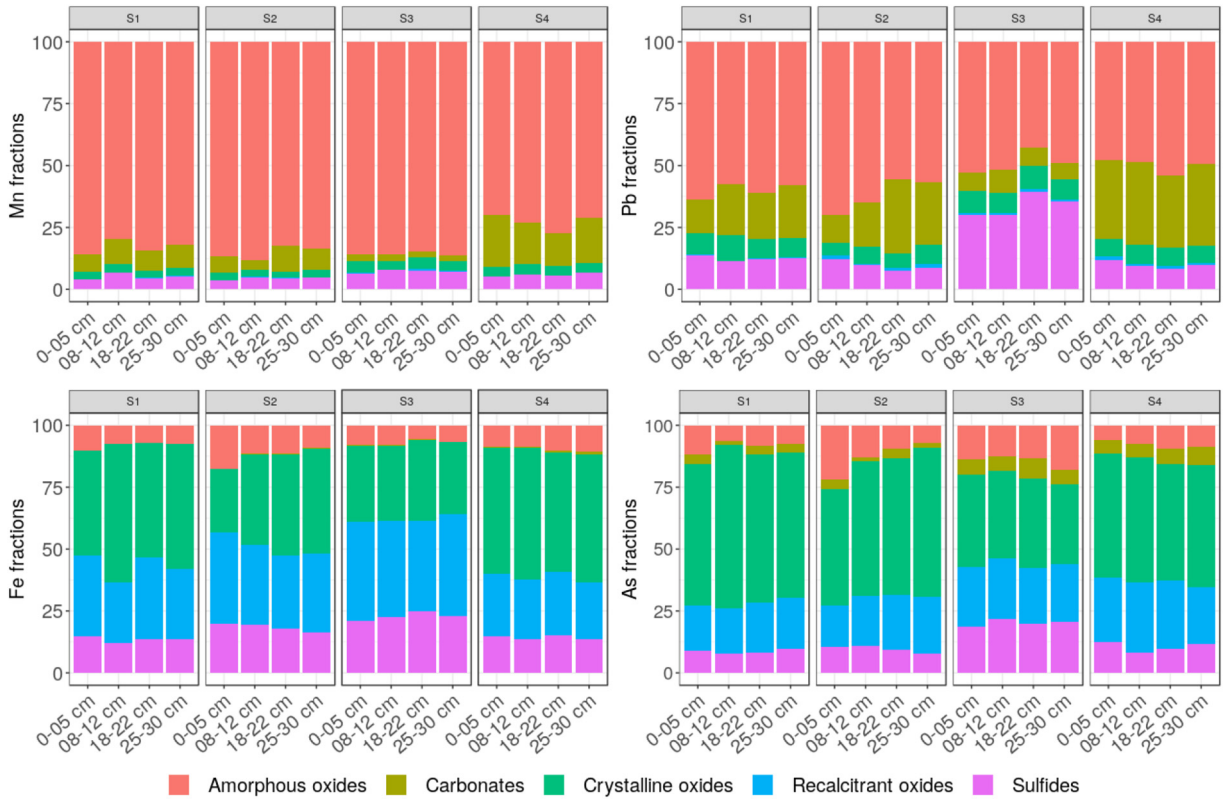

Fig. 5. Distribution percentages of Mn, Pb, As and Fe species in the extraction fluids from samples collected at different depths in the investigated sites: both Mn and Pb are found mostly in amorphous oxides, Fe both in crystalline and recalcitrant oxides and As mostly in crystalline oxides.

accumulate in the human brain through direct inhalation of dusts (Maher et al., 2016).

3.4. Manganese bioavailability

The prevalence of Mn in different phases could have significant implications to its bioavailability. Most of the Mn in the soils (Fig. 8), was not efficiently extracted in bioavailability extractions simulating digestion (gastric and intestinal extractions) and inhalation (lysosomal fluid and Gamble's Solution), however there were significant differences between extracted metal concentrations for contaminated samples. All extractions dissolved less than 5% of total Mn, relative contributions were variable and not significantly correlated with depth or site. Gastric-like extractions generally dissolved more Mn than intestinal fluids, and both extracted more than simulated lysosomal fluids, which represented at least 98% of all Mn extracted in inhalation-like extractions. Although the fractions of Mn extracted are reasonably low, the concentrations that could result from dissolution could still significantly impact health because the soils of the impacted sites S1, S2 and S3 all contain abundant Mn (more than 1000 mg Mn/kg). Alternatively, this could indicate that the documented toxic effects

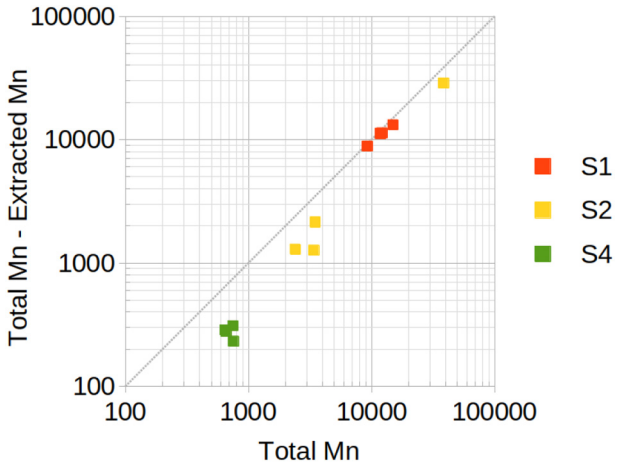

Fig. 6. Total (pXRF-measured) Mn versus unextracted Mn concentrations in S1 and S2, the most impacted sites, and in the control site S4.

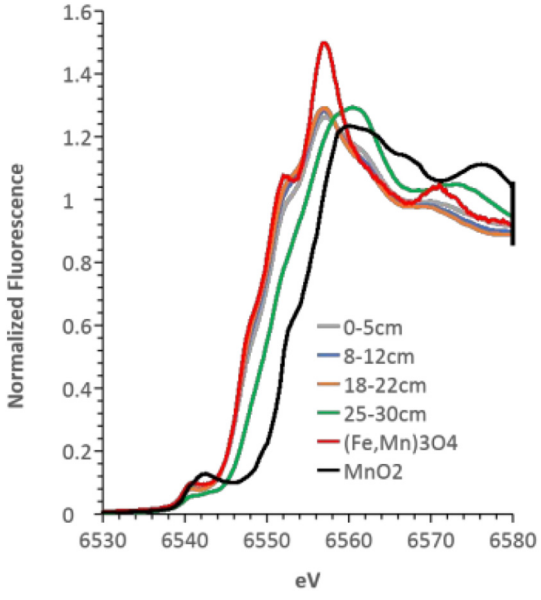

Fig. 7. Manganese XANES spectra of a soil profile from the contaminated soil profile S2. Spectra for samples collected from 0 to 20 cm are all similar to Mn substituted $(Fe,Mn)_3O_4$, while spectra of the deepest sample (25–30 cm) is oxidized, similar to other soils, though still distinct from MnO_2.

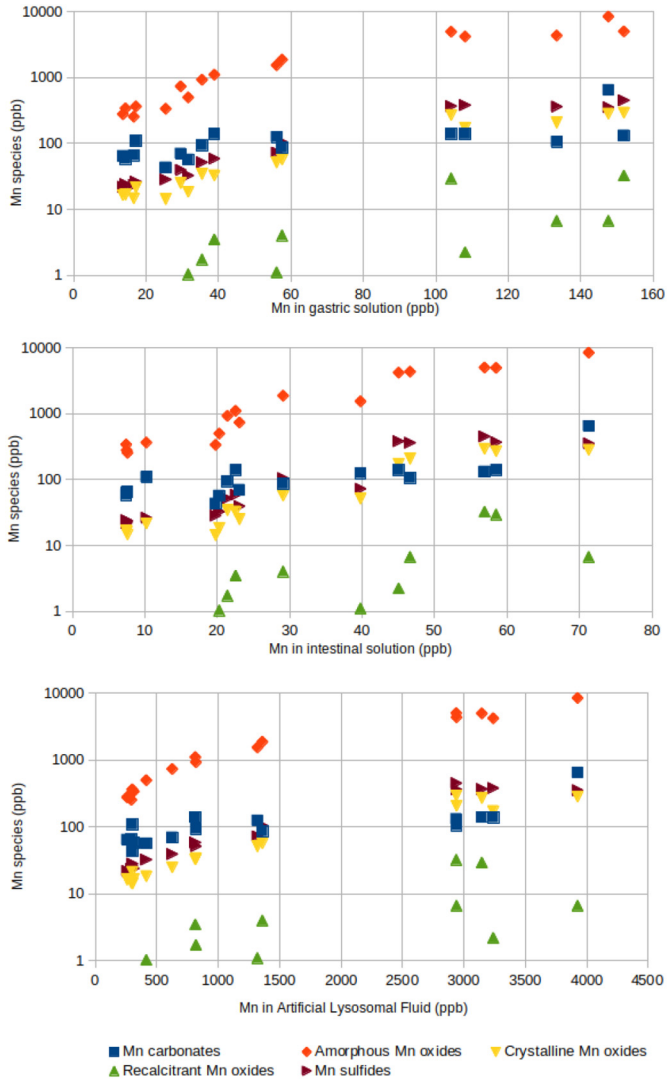

Fig. 8. Correlation plots between values of Mn extracted with the bio-accessibility extractions and with the sequential chemical extraction procedure.

of Mn are not due to dissolution but instead are a result of the direct interaction of mineral particulates with the lungs or gastrointestinal tract upon inhalation or ingestion.

4. Conclusions

In the soils near the ferroalloy plant of Bagnolo Mella, Italy, atmospherically-derived contamination is extensive in the top 15 cm of soils. Manganese, Zn, Cu, Pb, Ni and As all have concentrations that decrease with depth, despite their relative insolubility. In the case of Mn, this occurs despite the Mn being associated with recalcitrant $(Mn,Fe)_3O_4$ mineral form uniquely found in aerosols and unusual in soils. The contaminants, including Mn in magnetite, are redistributed in the soil by adsorption physical mixing or, potentially, colloid transport. Chemical transport is less likely because the elements are insoluble and the repartitioning to soil minerals would further decrease aqueous concentrations. This downward transport/repartitioning could affect soil toxicity. In the case of Pb, surface soil concentrations observed in urban soils are considered to be slightly toxic, because they retain Pb and enough of that Pb is bioavailable to impact humans. This could also be the case in Bagnolo Mella where the original, deposited mineral form $(Fe,Mn)_3O_4$ highlights the legacy of ferroalloy steel production. This mineral is insoluble and appears to have a low bioavailability, but that may represent an underestimate of the toxicity of these minerals because it does not account for direct interactions of the solid phase with the body. The relative persistence of $(Fe,Mn)_3O_4$ implies that it represents a potential long-term exposure risk, and that risk is primarily associated with the resuspension of surface soil particles in dust. In fact, aerosol $(Fe,Mn)_3O_4$ produced in combustion are particles with a diameter of a few nm (Maher et al., 2016), while most natural Mn minerals formed in soil form large aggregates (Hickey et al., 2008), but are much more soluble, bioavailable and yet are considered non-toxic. These results are transferable to other sites of contamination from ferroalloy emission and should suggest an intervention to reduce health risk in the local population because, although the bioavailable Mn fractions are reasonably low, they could result in significant concentration as the impacted sites all contain abundant Mn.

CRediT authorship contribution statement

Marco Peli: Conceptualization, Investigation, Data curation, Writing - original draft, Writing - review & editing. **Benjamin C. Bostick:** Methodology, Resources, Writing - review & editing. **Stefano Barontini:** Conceptualization, Methodology, Resources, Writing - original draft, Writing - review & editing. **Roberto G. Lucchini:** Supervision, Funding acquisition, Writing - review & editing. **Roberto Ranzi:** Methodology, Supervision, Funding acquisition, Writing - review & editing.

Declaration of competing interest

The authors declare that they have no known competing financial interests or personal relationships that could have appeared to influence the work reported in this paper.

Acknowledgements

The study was supported by the the University of Brescia (grant UNBSCLE 9015); by the European Union through its Sixth Framework Program for RTD (grant FOODCT- 2006–016253): it reflects only the authors' views, and the European Commission is not liable for any use that may be made of the information contained therein; by the National Institute of Environmental Health Sciences (NIEHS) (grants R01 ES019222, P30 ES023515): the content is solely the responsibility of the authors and does not necessarily represent the official views of the NIEHS or the National Institutes of Health; and by the Società Idrologica Italiana – Italian Hydrological Society (award *Premio Florisa Melone 2019*). This is LDEO Contribution Number 8455. The authors would like to thank the anonymous reviewer(s) for the constructive comments and suggestions, which improved the final version of this manuscript.

Appendix A. Supplementary data

Supplementary data to this article can be found online at https://doi.org/10.1016/j.scitotenv.2020.143123.

References

Basta, N.T., Gradwohl, R., Snethen, K.L., Schroder, J.L., 2001. Chemical immobilization of lead, zinc, and cadmium in smelter-contaminated soils using biosolids and rock phosphate. J. Environ. Qual. 30 (4), 1222–1230. https://doi.org/10.2134/jeq2001.3041222x.

Blume, H., Brümmer, G., Fleige, H., Horn, R., Kandeler, E., Kögel-Knabner, I., Kretzschmar, R., Stahr, K., Wilke, B.M., 2016. Scheffer/Schachtschabel Soil Science. Springer Berlin Heidelberg https://doi.org/10.1007/978-3-642-30942-7.

van den Boogaart, K. G., Tolosana-Delgado, R., Bren, M. (2019). Compositions: compositional data analysis, R package version 1.40–3.

Borgese, L., Federici, S., Zacco, A., Gianoncelli, A., Rizzo, L., Smith, D.R., Donna, F., Lucchini, R., Depero, L.E., Bontempi, E., 2013. Metal fractionation in soils andassessment of environmental contamination in Vallecamonica, Italy. Environ.Sci. Pollut. Res. 20 (7), 5067–5075. https://doi.org/10.1007/s11356-013-1473-8.

Boudissa, S.M., Lambert, J., Muller, C., Kennedy, G., Gareau, L., Zayed, J., 2006. Manganese concentrations in the soil and air in the vicinity of a closed manganese alloy production plant. Sci. Total Environ. 361 (1–3), 67–72. https://doi.org/10.1016/j.scitotenv.2018.01.246.

Carter, M.R., Gaudet, B.J., Stauffer, D.R., White, T.S., Brantley, S.L., 2015. Using soil records with atmospheric dispersion modeling to investigate the effects of clean air regulations on 60 years of manganese deposition in Marietta, Ohio (USA). Sci. Total Environ. 515-516, 49–59. https://doi.org/10.1016/j.scitotenv.2015.01.015.

Davidson, C.M., Urquhart, G.J., Ajmone-Marsan, F., Biasioli, M., da Costa Duarte, A., Díaz-Barrientos, E., Grcman, H., Hossack, L., Hursthouse, A.S., Madrid, L., Rodrigues, S., Zupan, M., 2006. Fractionation of potentially toxic elements in urban soils from five european cities by means of a harmonised sequential extraction procedure. Anal. Chim. Acta 565 (1), 63–72. https://doi.org/10.1016/j.aca.2006.02.014.

Dixit, S., Hering, J.G., 2003. Comparison of arsenic (V) and arsenic (III) sorption onto ironoxide minerals: implications for arsenic mobility. Environ. Sci. Technol. 37, 4182–4189. https://doi.org/10.1021/es030309t.

Eastman, R.R., Jursa, T.P., Benedetti, C., Lucchini, R.G., Smith, D.R., 2013. Hair as a biomarker of environmental manganese exposure. Environ. Sci. Technol 47 (3), 1629–1637. https://doi.org/10.1021/es3035297.

Ferri, R., Hashim, D., Smith, D.R., Guazzetti, S., Donna, F., Ferretti, E., Curatolo, M., Moneta, C., Beone, G.M., Lucchini, R.G., 2015. Metal contamination of home garden soils and cultivated vegetables in the province of Brescia, Italy: implications for human exposure. Sci. Total Environ. 518, 507–517. https://doi.org/10.1016/j.scitotenv.2015.02.072.

Filzmoser, P., Hron, K., Reimann, C., 2009. Principal component analysis for compositional data with outliers. Environmetrics 20 (6), 621–632. https://doi.org/10.1002/env.966.

Fulk, F., Succop, P., Hilbert, T.J., Beidler, C., Brown, D., Reponen, T., Haynes, E.N., 2017. Pathways of inhalation exposure to manganese in children living near a ferromanganese refinery: a structural equation modeling approach. Sci. Total Environ. 579, 768–775. https://doi.org/10.1016/j.scitotenv.2016.11.030.

Herndon, E.M., Jin, L.J., Brantley, S.L., 2011. Soils reveal widespread manganese enrichment from industrial inputs. Environ. Sci. Technol. 45 (1), 241–247. https://doi.org/10.1021/es102001w.

Hickey, P.J., McDaniel, P.A., Strawn, D.G., 2008. Characterization of iron- and manganese-cemented redoximorphic aggregates in wetland soils contaminated with mine wastes. J. Environ. Qual. 37, 2375–2385. https://doi.org/10.2134/jeq2007.0488.

Hošek, M., Matys Grygar, T., Elznicová, J., Faměra, M., Popelka, J., Matkovič, J., Kiss, T., 2018. Geochemical mapping in polluted floodplains using in situ X-ray fluorescence analysis, geophysical imaging, and statistics: surprising complexity of floodplain pollution hotspot. Catena 171, 632–644. https://doi.org/10.1016/j.catena.2018.07.037.

Huang, Z., Tang, Y., Zhang, K., Chen, Y., Wang, Y., Kong, L., You, T., Gu, Z., 2016. Environmental risk assessment of manganese and its associated heavy metals in a stream impacted by manganese mining in South China. Hum. Ecol. Risk. Assess. 22 (6), 1341–1358. https://doi.org/10.1080/10807039.2016.1169915.

Kaste, J.M., Bostick, B.C., Heimsath, A.M., Steinnes, E., Friedland, A.J., 2011. Using atmospheric fallout to date O horizon layers and quantify metal dynamics during decomposition. Geochim. Cosmochim. Acta 75, 1642–1661. https://doi.org/10.1016/j.gca.2011.01.011.

Lambert, T.W., Lane, S., 2004. Lead, arsenic, and polycyclic aromatic hydrocarbons in soil and house dust in the communities surrounding the Sydney, Nova Scotia, tar ponds. Environ. Health Perspect. 112 (1), 35–41. https://doi.org/10.1289/ehp.6423.

Layton, D.W., Beamer, P.I., 2009. Migration of contaminated soil and airborne particulates to indoor dust. Environ. Sci. Technol. 43 (21), 8199–8205. https://doi.org/10.1021/es9003735.

Liang, X.L., He, Z.S., Wei, G.L., Liu, P., Zhong, Y.H., Tan, W., Du, P.X., Zhu, J.X., He, H.P., Zhang, J., 2014. The distinct effects of Mn substitution on the reactivity of magnetite in heterogeneous Fenton reaction and Pb(II) adsorption. J. Colloid Interface Sci. 426, 181–189. https://doi.org/10.1016/j.jcis.2014.03.065.

Lucchini, R., Placidi, D., Cagna, G., Fedrighi, C., Oppini, M., Peli, M., Zoni, S., 2017. Manganese and developmental neurotoxicity. In: Aschner, M., Costa, L.G. (Eds.), *Neurotoxicity of Metals*, Advances in Neurobiology 18. vol. 2017, pp. 13–34. https://doi.org/10.1007/978-3-319-60189-2_2 Springer International Publishing AG.

Maher, B.A., 2019. Airborne magnetite- and iron-rich pollution nanoparticles: potential neurotoxicants and environmental risk factors for neurodegenerative disease, including alzheimer's disease. J. Alzheim. Dis. 71, 361–375. https://doi.org/10.3233/JAD-190204.

Maher, B.A., Ahmed, I.A.M., Karloukovski, V., MacLaren, D.A., Foulds, P.G., Allsop, D., Mann, D.M.A., Calderon-Garciduenas, L., 2016. Magnetite pollution nanoparticles in the human brain. Proc. Natl. Acad. Sci. U. S. A. 113 (39), 10797—10801. https://doi.org/10.1073/pnas.1605941113.

Mamut, A., Eziz, M., Mohammad, A., 2018. Pollution and ecological risk assessment of heavy metals in farmland soils in Yanqi County, Xinjiang, northwest China. Eurasian Soil Sci 51 (8), 985–993. https://doi.org/10.1134/S1064229318080082.

Miah, M.R., Ijomone, O.M., Okoh, C.O.A., Ijomone, O.K., Akingbade, G.T., Ke, T., Krum, B., da Cunha Martins Jr., A., Akinyemi, A., Aranoff, N., Antunes Soares, F.A., Bowman, A.B., Aschner, M., 2020. The effects of manganese overexposure on brain health. Neurochem. Int. 135, 104688. https://doi.org/10.1016/j.neuint.2020.104688.

Otero-Pregigueiro, D., Hernández-Pellón, A., Borge, R., Fernández-Olmo, I., 2018. Estimation of PM10-bound manganese concentration near a ferromanganese alloy plant by atmospheric dispersion modelling. Sci. Total Environ. 627, 534–543. https://doi.org/10.1016/j.scitotenv.2018.01.246.

Pavilonis, B.T., Lioy, P.J., Guazzetti, S., Bostick, B.C., Donna, F., Peli, M., Zimmerman, N.J., Bertrand, P., Lucas, E., Smith, D.R., Georgopoulos, P.G., Mi, Z., Royce, S.G., Lucchini, R.G., 2015. Manganese concentrations in soil and settled dust in an area with historic ferroalloy production. J. Expo. Sci. Environ. Epidemiol. 25 (4), 443–450. https://doi.org/10.1038/jes.2014.70.

R Core Team (2018). R: A Language and Environment for Statistical Computing. RFoundation for Statistical Computing, Vienna, Austria https://www.R-project.org/.

Reimann, C., Fabian, K., Birke, M., Filzmoser, P., Demetriades, A., Négrel, P., Oorts, K., Matschullat, J., de Caritat, P., The GEMAS Project Team, 2018. GEMAS: establishing geochemical background and threshold for 53 chemical elements in European agricultural soil. Appl. Geochem. 88, 302–318. https://doi.org/10.1016/j.apgeochem.2017.01.021.

Rico, M.I., Alvarez, J.M., Lopez-Valdivia, L.M., Novillo, J., Obrador, A., 2009. Manganese and zinc in acidic agricultural soils from Central Spain: distribution and phytoavailability prediction with chemical extraction tests. Soil Sci. 174 (2), 94–104. https://doi.org/10.1097/SS.0b013e3181975058.

Rodriguez, L., Ruiz, E., Alonso-Azcarate, J., Rincon, J., 2009. Heavy metal distribution and chemical speciation in tailings and soils around a Pb–Zn mine in Spain. J. Environ. Manag. 90 (2), 1106–1116. https://doi.org/10.1016/j.jenvman.2008.04.007.

Sparks, D.L., Page, A.L., Helmke, P.A., Loeppert, R.H., Soltanpour, P.N., Tabatabai, M.A., Johnston, C.T., Sumner, M.E., 1996. Methods of soil analysis, SSSA book series. Soil Science Society of America, American Society of Agronomy. https://doi.org/10.2136/sssabookser5.3.

Stockmann, U., Cattle, S.R., Minasny, B., McBratney, A.B., 2016. Utilizing portable X—ray fluorescence spectrometry for in-field investigation of pedogenesis. Catena 139, 220–231. https://doi.org/10.1016/j.catena.2016.01.007.

Sun, J., Chillrud, S.N., Mailloux, B.J., Bostick, B.C., 2016a. In situ magnetite formation and long–term arsenic immobilization under advective flow conditions. Environ. Sci. Technol 50 (18), 10162–10171. https://doi.org/10.1021/acs.est.6b02362.

Sun, J., Chillrud, S.N., Mailloux, B.J., Stute, M., Singh, R., Dong, H., Lepre, C.J., Bostick, B.C., 2016b. Enhanced and stabilized arsenic retention in microcosms through the microbial oxidation of ferrous Iron by nitrate. Chemosphere 144, 1106–1115. https://doi.org/10.1016/j.chemosphere.2015.09.045.

Sun, J., Yu, R., Hu, G., Su, G., Zhang, Y., 2018. Tracing of heavy metal sources and mobility in a soil depth profile via isotopic variation of Pb and Sr. Catena 71, 440–449. https://doi.org/10.1016/j.catena.2018.07.040.

Trueman, B.F., Gregory, B., McCormick, N.E., Gao, Y., Gora, S., Anaviapik-Soucie, T., L'Herault, V., Gagnon, G.A., 2019. Manganese increases lead release to drinking water. Environ. Sci. Technol. 53 (9), 4803–4812. https://doi.org/10.1021/acs.est.9b00317.

Tume, P., Gonzalez, E., Reyes, F., Fuentes, J.P., Roca, N., Bech, J., Medina, G., 2019. Sources analysis and health risk assessment of trace elements in urban soils of Hualpen, Chile. Catena 175, 304–316. https://doi.org/10.1016/j.catena.2018.12.030.

Urrutia-Goyes, R., Argyraki, A., Ornelas-Soto, N., 2017. Assessing lead, nickel, and zinc pollution in topsoil from a historic shooting range rehabilitated into a public urban park. Int. J. Environ. Res. Public Health 14 (7). https://doi.org/10.3390/ijerph14070698.

Villalobos, M., Bargar, J., Sposito, G., 2005. Mechanisms of Pb(II) sorption on a biogenic manganese oxide. Environ. Sci. Technol. 39 (2), 569–576. https://doi.org/10.1021/es049434a.

Zereini, F., Wiseman, C.L.S., Puettmann, W., 2012. In vitro investigations of platinum, palladium, and rhodium mobility in urban airborne particulate matter (PM10, PM2.5, and PM1) using simulated lung fluids. Environ. Sci. Technol 46 (18), 10326–10333. https://doi.org/10.1021/es3020887.